The Journal of Adhesion, 92:18–38, 2016

ISSN: 0021-8464 print/1545-5823 online
DOI: 10.1080/00218464.2014.987867

Taylor & Francis
Taylor & Francis Group

Adhesion Reduction of Diamond-Like Carbon Films Based on Different Contact Geometries by Using an AFM

TIANMAO LAI[1], PING HUANG[1], and YAZHI CAI[2]

[1]*School of Mechanical and Automotive Engineering, South China University of Technology, Guangzhou, Guangdong, China*
[2]*Xin Platinum Hardware Technology Company Limited, Dongguan, China*

The effect of reducing adhesion force by coating with a metal-containing diamond-like carbon (DLC) film has been studied by recording force–displacement curves with an atomic force microscope. A flat tip, a spherical tip, and some sharp tips were applied to mimic the different contact geometries. The results show that both under ambient conditions and in dry nitrogen, the DLC film can effectively reduce the adhesion force for different contact geometries. The reduction of the adhesion force was attributed to the decrease of the surface free energy and the increase of the contact angle for water. The reduction ratio of adhesion is closely related to contact geometry, the roughness of DLC film, material characteristics paired with DLC film and the environment. These factors are mutually coupled to determine the final reduction ratio. Under both conditions, the DLC film also plays a role in reducing the wear and tear when measuring the adhesion forces.

KEYWORDS *Atomic force microscopy; Coatings; Force–displacement curve; Particle adhesion; Wear; X-ray photoelectron spectroscopy*

Received 17 September 2014; in final form 11 November 2014.

Address correspondence to Tianmao Lai, School of Mechanical and Automotive Engineering, South China University of Technology, Room 403, Building 19, Wushan Road 381, Tianhe, Guangzhou, Guangdong 510640, China, E-mail: laitianmao@163.com

Color versions of one or more of the figures in the article can be found online at www.tandfonline.com/gadh.

1. INTRODUCTION

With the increasing shrink of miniaturized systems, such as micro-/nano-electromechanical systems (MEMS/NEMS) and magnetic storage devices, the adhesion in the micro-scale and nano-scale becomes more and more important. For small-scale mechanical systems, the surface effect becomes the dominant factor influencing mechanical performance due to a high surface-area-to-volume ratio [1]. As a consequence, the influence of the adhesion on the reliability of these systems becomes significant. The adhesion force is the dominant factor of the failures of MEMS in the manufacture and in use [2]. Therefore, it is urgent to reduce the adhesion force to further practicability and miniaturization of MEMS.

In the most general case, the adhesion force is a combination of the electrostatic force, the van der Waals (vdW) force, the capillary force, and forces due to chemical bonds or acid–base interactions [3]. Under different conditions, the dominant factors of adhesion may be different. Under ambient conditions, the capillary force is always present due to capillary condensation and adsorption of thin water films on surfaces. This interaction depends on the relative humidity and the hydrophilicity of the surfaces. In dry gaseous environments, the capillary force will disappear, and the vdW force and electrostatic forces may become the dominant forces. In particular, the electrostatic forces can be large on insulators, since the charge dissipation is ineffective at low humidity. Under distilled water, in general, there are no capillary force and electrostatic force. And the significant contribution is from the vdW force.

It is well-known that the increase of roughness will reduce the real contact area, resulting in lower adhesion force. Surface-texturing modification is to design the surface structure such as dimples, grooves, or channels with controlled geometry on the surface of mechanical components. It has long been recognized that surface-texturing is an effective approach to reduce the contact area between surfaces and ultimately reduce the adhesion [4,5]. However, the micro-structures may increase wear and tear, and cause the water vapor in the air condense into the structure to form liquid bridges, leading to larger capillary forces. Moreover, some components are not appropriate for the design of micro-structures. Therefore, the method of reducing adhesion by the micro-structures appears to have little effect.

The adhesion force is directly proportional to the work of adhesion. The work of adhesion is related to the surface energy. Therefore, the decrease of the surface energy will be an effective method to reduce the adhesion. The chemical modification of the surfaces should be achieved to reduce the surface energy. There are some methods. The surface can be terminated with hydrogen, or coated with thin organic films, or coated with fluorocarbon films [6]. In addition, some hard coatings can be used to reduce adhesion,

such as silicon carbide, carbon nitride and diamond-like carbon (DLC) film. The DLC film is an amorphous carbon material, and consists of the sp^3C bonding (diamond structure) and sp^2C bonding (graphite structure). The DLC film is widely applied due to its favorable nature such as high hardness, high wear resistance, low friction coefficient, and chemical inertness.

In order to reduce the adhesion force, measuring the adhesion force is necessary in advance. There are many apparatuses to measure adhesion at the microscopic scale, such as, surface force apparatus (SFA), interfacial force microscope (IFM), and atomic force microscopy (AFM), and so on. Among them, the AFM has been commonly used for the investigation of adhesion in the micro-/nano-scale. By using an AFM, it is simple and accurate to determine adhesion forces with high spatial resolution. Adhesion forces between any types of surfaces can be measured in any environment. And the AFM is less subject to contamination than other apparatuses measuring adhesion in the micro-scale. The adhesion force is determined by recording a force–displacement curve. The force–displacement curve is obtained by monitoring the deflection of a cantilever as the tip approaches and retracts from the sample surface.

Since the DLC film is widely applied in the MEMS, the detail of the reduction mechanism should be considered. However, there are only a few studies concerning the adhesion reduction of the DLC film. For example, Houston *et al.* [7] reported that the adhesion forces were reduced on DLC surfaces by about a factor of five compared to that on cleaned silicon surfaces. In the absence of meniscus forces, the adhesion force was expected to decrease by over an order of magnitude between two DLC-coated surfaces. Liu and Bhushan [8] used a micro-triboapparatus to investigate the tribological properties of the materials commonly used in MEMS. They found that the use of DLC film can apparently reduce the adhesion force of Si (100) in a whole testing range. Gou *et al.* [9] investigated the characters of the DLC films deposited on silicon probes by plasma-enhanced chemical vapor deposition (PECVD). They found that the adhesion force was reduced by the DLC film under ambient conditions. Although it is well-accepted that the adhesion force can be reduced by coating a DLC film, there are still two some questions needing discussion, since many factors can influence the adhesion, such as surface roughness, hydrophilicity, temperature, and humidity. The first one is what should be attributed to for the reduction of adhesion. The second is whether the adhesion force will be reduced under all conditions, like different contact geometries or different environments. Therefore, the discussion of the reduction mechanism of the adhesion is still necessary.

In this paper, the effect of reducing adhesion force by the DLC film coating were studied by recording force–displacement curves with an AFM. The experiments were carried out both under ambient conditions and in dry nitrogen. A flat tip, a spherical tip, and some sharp tips were applied to mimic

the different contact geometries. The chemical composition of the film was analyzed by Raman spectroscopy and X-ray photoelectron spectroscopy (XPS). The free energies of the samples were calculated by the contact angles between the probe liquids and the surfaces. Many locations on the sample were selected to record force–displacement curves with different kinds of tips. The adhesion distribution for each contact geometry was discussed. The effect of adhesion reduction was compared between different contact geometries and between different conditions. Also, the wear of the sharp tips was studied. These experimental results can provide a helpful reference to the design and manufacture of micro-nano-devices and instruments.

2. EXPERIMENTAL

2.1. Sample Preparation

There were four samples used in the experiments. Sample 1 (polished Si) is an N-type polished silicon wafer of (100) orientation. The thickness of it is $400 \pm 10\,\mu m$, and the resistivity is 5–10 Ω cm. The sample was cleaned by the hydrofluoric acid (HF) to remove the natural oxide layer on the sample. Sample 2 (grooved Si) was grinded from the polished Si by a grinding wheel with diamond particles [10]. Sample 3 (DLC-coated polished Si) and sample 4 (DLC-coated grooved Si) were obtained from sample 1 and sample 2 by coating with a layer of the DLC film.

The DLC film is a multilayered metal-containing DLC film. It was obtained by the method of magnetron sputtering physical vapor deposition (MSPVD). The samples were ultrasonically cleaned in an alcohol solution for 15 min, and then ultrasonically cleaned in distilled water for 15 min. The substrates were placed in a rotary sample holder after drying. In order to remove the water thin film on the sample and increase the binding force between the film and the substrates, the samples were baked in a chamber at 220°C for about 60 min. The background pressure in the sputtering chamber was pumped below 9×10^{-3} Pa before sputtering gases were introduced. The coating thickness was controlled by the deposition time. The samples were first coated with titanium (Ti) for 5 min, then the amorphous structure of Ti and tungsten carbide (WC) for 30 min, then the WC and acetylene (carbon source) for 45 min.

The scanning electron microscope (SEM) image of the section of DLC-coated polished Si is shown in Fig. 1. It was determined by using a SEM (Zeiss MERLIN Field Emission SEM, Carl Zeiss NTS GmbH, Oberkochen, Germany). It can be observed that the honeycomb structure of the DLC film is very different from the structure of Si. The thickness of the film is ~1 μm. Since the DLC film on the grooved Si is obtained in the same batch, the thickness of it is viewed also as ~1 μm.

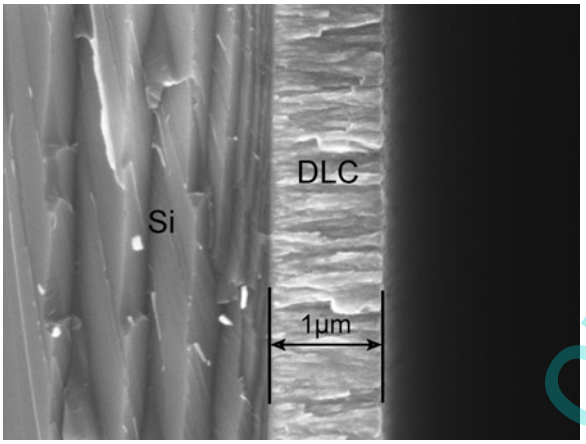

FIGURE 1 SEM image of the section of DLC-coated polished Si.

2.2. Adhesion Measurement Method

The measurements of adhesion forces were performed by using an atomic force microscope of beam deflection type (AFM, Being Nano-Instruments CSPM-4000, Guangzhou, China). The microscope can be operated under ambient conditions and in a nitrogen-filled glove box (Etelux Lab2000, Etelux Inert Gas System Company Limited, Beijing, China) where the water content and oxygen content can all be less than 0.1 ppm.

Four types of AFM probes were used to measure the adhesion force in this study. As shown in Fig. 2, the tip shapes of the probes were determined by using the SEM mentioned above. The first one (flat tip) is a single

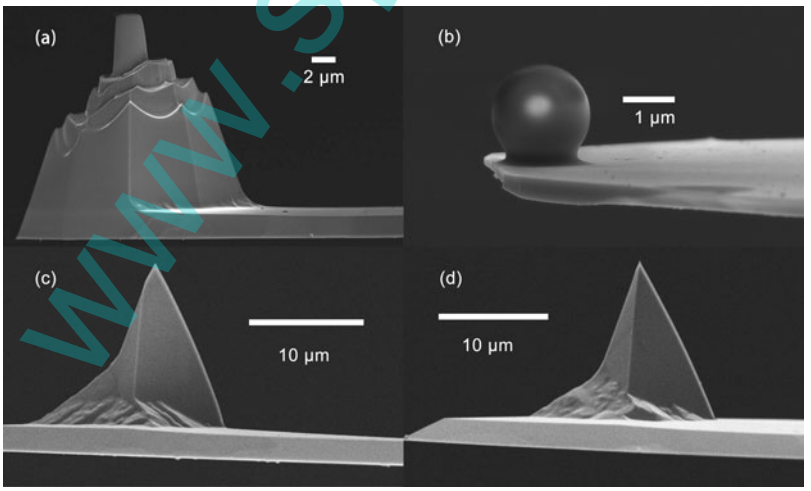

FIGURE 2 Scanning electron microscope images of the tips: (a) flat tip, (b) spherical tip, (c) sharp tip #1, and (d) DLC-coated sharp tip #1.

crystalline silicon probe (PL2-CONTR, Nanosensors, Neuchatel, Switzerland). As shown in Fig. 2(a), an intentionally blunt tip with a well-defined circular end-face is located at the free end of a rectangular cantilever. The flat tip is formed by focused ion beam milling and has a ~1.73 μm diameter contact area. The second one (spherical tip) is shown in Fig. 2(b). A spherical SiO_2 particle with diameter ~1.9 μm is attached to the end of a cantilever (Novascan Technologies, Ames, IA USA). The third type (ContAl, Budget Sensors, Innovative Solutions Bulgaria Limited, Sofia, Bulgaria) and the fourth type (ContDLC, Budget Sensors, Innovative Solutions Bulgaria Limited, Sofia, Bulgaria) are all rotated monolithic silicon probes. Since sharp tips wear easily, two probes of the third type (sharp silicon tip #1 and #2) and three probes of the fourth type (sharp DLC-coated tip #1, #2, and #3) were used here. The sharp silicon tip #1 and the sharp DLC-coated tip #1 are shown in Figs. 2(c) and 2(d), respectively. The tips of the fourth type are coated with a layer of the DLC film (the cantilevers are not). As quoted by the manufacturers, the tips of the third and fourth types have parabolic shapes with end radiuses <10 and <15 nm, respectively. However, the exact radius measured by the SEM was quite different from the nominal one. In the process of collecting force–displacement curves, sharp tips wear gradually. Therefore, the end radius is not a controllable parameter and the experimental procedure (first collecting curves on the Si wafer or the DLC-coated one) will influence the outcomes. That is why 2 or 3 sharp tips of the same type were used in this study. Since the tip end radiuses of the same type are different from each other and the shape of the sharp tip changes gradually, the radiuses of the sharp tips are unable to be supplied in this study. Therefore, the adhesion forces measured by different sharp tips will not be compared with each other. That is, the adhesion forces measured by the same tip will be compared with each other to study the adhesion reduction of the DLC film.

The spring constants of the cantilevers mentioned above were obtained with the thermal tune methods by using an AFM (MFP-3D Classic, Asylum Research, Santa Barbara, CA, USA). For each probe, the virtual deflection was first determined by collecting a force–displacement curve when the tip was still far away from the surface (the entire range of the scanner movement in Z-direction). The virtual deflection is a mechanical coupling of the deflection signal with the Z-direction movement. After the virtual deflection was obtained, the slight slope in the force–displacement curve will be canceled out. Then another force–distance curve should be collected. This time, the tip was touched with a hard substrate (cleaned Al_2O_3). From the curve, the slope of the contact region should be measured and the inverse optical lever sensitivity (in units of nm/V) would be given. By performing a thermal tune, a thermal power spectral density (PSD) plot would be obtained. At last, the spring constant would be given by a successful fitting of the simple harmonic oscillator (SHO) equation on the first resonance peak. It should be noted that

the deflection on the photodetector should be adjusted to zero before a thermal tune. As quoted by the manufacturers, the spring constants of the cantilevers with flat and spherical tips are 0.11 and 0.6 N/m, respectively. However, by using the thermal tune methods, the spring constants of them were 0.136 and 0.591 N/m, respectively. The spring constants of cantilevers with sharp tips provided by the suppliers were all 0.2 N/m. However, by using the thermal tune methods, the spring constants of cantilevers with sharp silicon tip #1 and #2 were 0.239 and 0.244 N/m, respectively. And, the spring constants of cantilevers with sharp DLC-coated tips #1, #2, and #3 were 0.175, 0.156, and 0.182 N/m, respectively.

In the AFM, adhesion measurements were performed by recording force–displacement curves. A typical force–displacement curve is shown in Fig. 3. In the measurement, the probe tip is initially far away from the sample (A). The zero line is defined as a part of the force–displacement curve in which the tip exerts no force on the sample. The sample is then brought into contact with the stationary tip by the extension of the scanner. Upon approaching the surface, the tip may sense attractive forces or repulsive forces, which cause the end of the cantilever to bend downward or upward (not shown in Fig. 3). If the short-range attractive force gradient of the tip–sample interaction exceeds the normal spring constant of the cantilever, the tip will snap into contact with the sample (B). As the sample continues to move up, the cantilever further deflects until a maximum value is reached (C). Subsequently, the probe is retracted away from the sample. During this process, the tip keeps in contact with the sample because of the adhesion (D). When the normal spring constant overcomes the attractive force gradient, the cantilever snaps back to its original undeflected position (E). The adhesion force can be obtained by multiplying the normal spring constant

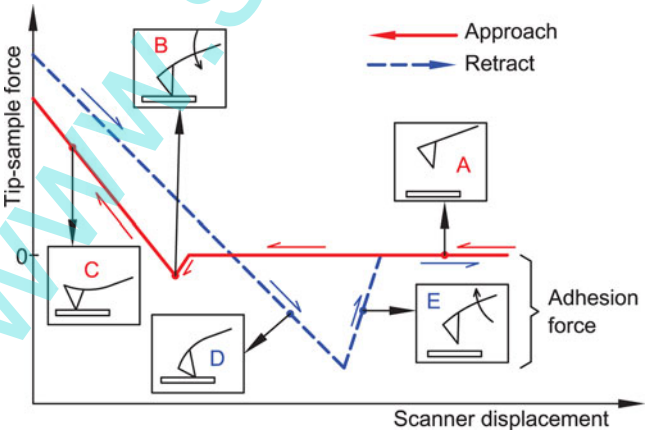

FIGURE 3 A schematic of a typical force–displacement curve with highlights of the various stages (A–E) of the tip as it is brought into and out of contact with the sample at a fixed location.

with the deflection which is continuously recorded as a function of scanner displacement.

2.3. Other Tests

Raman spectra of the DLC-coated polished Si and the DLC-coated sharp tip were also obtained. Raman spectra were collected from 600 to 3000 cm^{-1} on a LabRAM ARAMIS Raman spectrometer (LabRAM HORIBA Jobin Yvon, Edison, NJ) with a HeNe laser (laser wavelength $\lambda = 633$ nm, a laser power of 17 mW) as an excitation source. The chemical composition of the DLC film was measured with XPS. The XPS spectrum was recorded using a Kratos Axis Ultra spectrometer (Kratos Analytical, Manchester, UK) employing a monochromated Al Kα X-ray source (1486.6 eV) with resolution of 0.1 eV, hybrid (magnetic/electrostatic) optics, and a multichannel plate and delay line detector.

Contact angle measurement was conducted on OCA 40 Micro (DataPhysics Instruments GmbH, Filderstadt, Germany). Two probe liquids with different surface tensions and surface tension components (diiodomethane and distilled water) were used in these measurements. The contact angles were measured for at least five liquid drops having a base diameter from 4 to 6 mm. All measurements were conducted at room temperature, 23°C ± 1°C.

The pollution should be avoided when carrying out tests and experiments. Therefore, before all the tests and experiments (SEM, topography, Raman, XPS, contact angle, and adhesion and so on), the sample was ultrasonically cleaned in an alcohol solution for 15 min, and then ultrasonically cleaned in the distilled water for 15 min.

3. RESULTS AND DISCUSSION

3.1. Sample Surface Characterization: Raman Spectrum and XPS

Raman spectroscopy is a comparatively simple and nondestructive analysis technique. Raman spectra are usually used as indirect evidence of the film composition. The Raman spectrum of the DLC-coated polished Si is shown in Fig. 4(a). The resulting Raman spectrum is deconvoluted with Gaussian method. The spectrum has two peaks (D peak and G peak) between 1100 and 1800 cm^{-1} as shown in Fig. 4. It is the characteristic feature of the DLC film.

The Raman spectrum of the DLC film on the sharp tip is shown in Fig. 4(b). The spectrum consisted of a sharply peaked band at 950 cm^{-1} and a broadband at about 1550 cm^{-1}. The sharply peaked band is due to the second-order Raman spectrum of the underlying Si substrate. Since the thickness of the DLC film is only 15 nm, the laser will penetrate the film. The intensity of the 950 cm^{-1} band will increase with increasing sp^3 bonding due to its optical

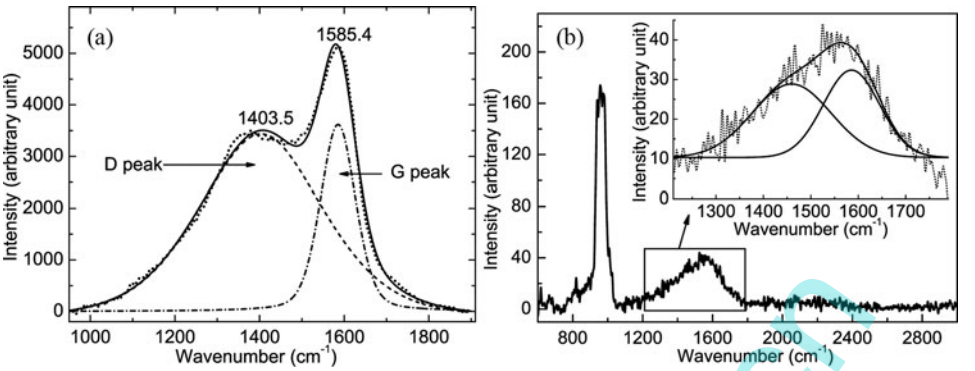

FIGURE 4 Raman spectrums of (a) the DLC-coated polished Si and (b) the DLC-coated sharp tip.

transparency, and disappears for the samples with primarily sp^2 bonding [11]. After fitting, we also find the characteristic peaks of the DLC film.

Since Raman spectroscopy is relatively unreliable in quantitative analysis of sp^3 content, XPS analysis was employed to get quantitative results of film composition. Figure 5(a) shows the full-scale XPS spectrum of the DLC-coated polished Si. Two sharp peaks of C1 s and O1 s are shown in the spectrum. The trace of O1 s was probably due to the contamination of the film surface after exposure to air. The trace of Ti and W (not marked in Fig. 5) was due to the accumulation during deposition.

The sp^3 fraction of DLC films was deduced from XPS fitting for C1 s core peak. Figure 5(b) indicates the deconvolution of C1 s peak spectrum. Each component is a convolution of a Gaussian and a Lorentzian method, and the contribution of the background was approximated by the Shirley method. The peak spectrum consists of peaks due to diamond (sp^3C, ~285.5 eV), graphite (sp^2C, ~284.2 eV), and C–O bonds or C=O bonds (~288.0 eV) phases. Since

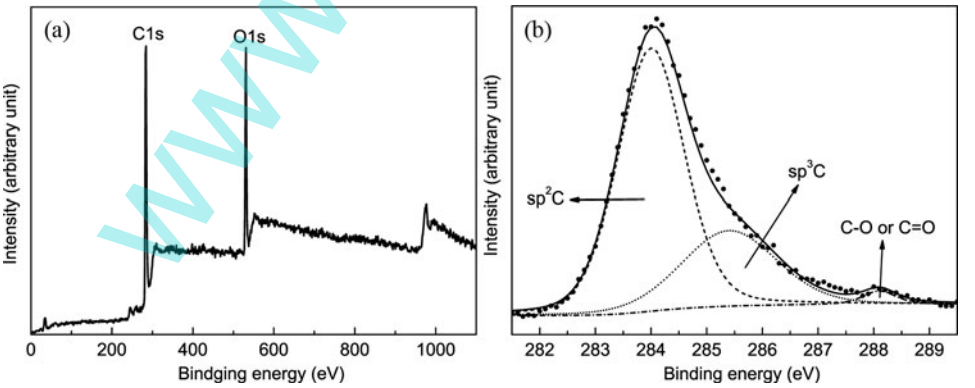

FIGURE 5 XPS spectrum of the DLC-coated polished Si: (a) full-scale spectrum and (b) the deconvolution of C1 s peak.

the area of each peak was directly related to the concentration of the corresponding, the sp^3 content was estimated by taking the ratio of diamond peak area over the sum of all the peak areas [12]. As a result, the presumable sp^3C content of the sample is ~28.6%. It should be noted that this determination method is really not very reliable [13]. Since the sp^3C content of the DLC film will not be compared with that of others, the estimated value is used here.

3.2. Sample Surface Characterization: Topographical Analysis

The surface topographies of the samples have been determined from an imaged area of 60 μm × 60 μm which are the representative of the samples, as shown in Fig. 6. A probe with tip radius less than 10 nm (Tap300Al-G, Budget Sensors, Innovative Solutions Bulgaria Limited, Sofia, Bulgaria) was used to measure the surface topographies by the tapping mode of the AFM. Its nominal vibration frequency is 300 kHz, and the nominal spring constant is 40 Nm^{-1}. The surface roughness is quantified using root mean square (RMS) roughness R_q. The parameter is defined by

$$R_q = \sqrt{\frac{1}{n}\left[\sum_{i=1}^{n}(z_i - z_{ave})^2\right]}, \tag{1}$$

where z_i is the topographic height at point i, n is the number of points measured within the area, z_{ave} is the average value of topographic heights

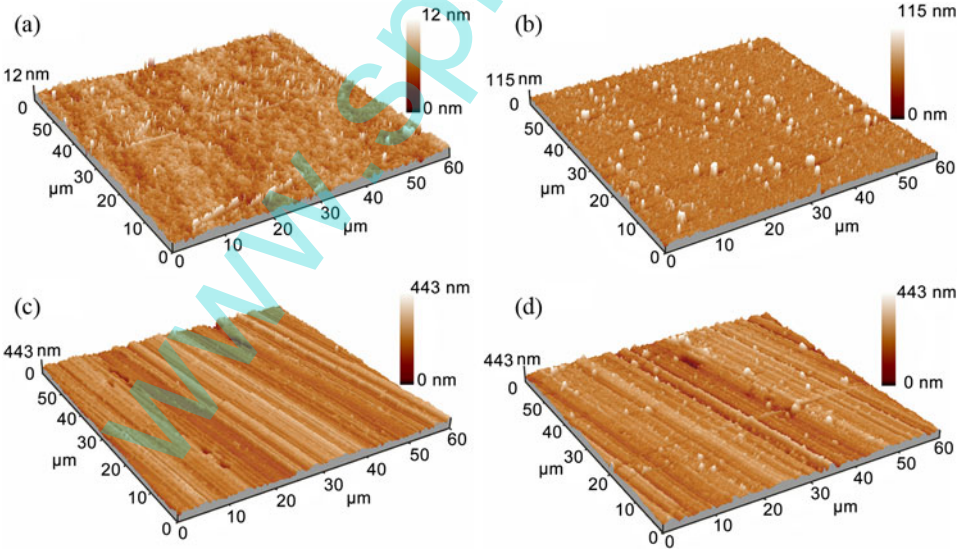

FIGURE 6 Topographic AFM images of all the samples: (a) polished Si, $R_q = 1.13$ nm, (b) DLC-coated polished Si, $R_q = 8.93$ nm, (c) grooved Si, $R_q = 36.6$ nm, and (d) DLC-coated grooved Si, $R_q = 40.9$ nm.

within the area, and $z_{ave} = \left(\sum_{i=1}^{n} z_i\right)/n$. The RMS roughness was determined from the images presented in Fig. 6 and found to be 1.13, 8.93, 36.6, and 40.9 nm, respectively. The surface height distributions of the samples are all Gaussian-like (not shown in Fig. 6). The results show that the roughness of the DLC-coated polished Si is eight times as large as that of the polished Si. This is primarily caused by some particles on the DLC film. The heights of the particles are about 50 nm. Since the groove Si is relatively rough, the influence of the particles on the DLC film can be nearly neglected.

3.3. Sample Surface Characterization: Surface Free Energy

The surface free energies of the surfaces were calculated by contact angles. The relationship between the contact angle and the surface tension is $\cos\theta = (\gamma_S - \gamma_{SL})\gamma_L$, where θ is the contact angle, γ_S and γ_L are solid and liquid surface tension, respectively, γ_{SL} is the solid–liquid interfacial tension. Fowkes [14] proposed that the surface tension can be decomposed into two components, $\gamma = \gamma^d + \gamma^p$, where γ^d and γ^p are the dispersive component and polar component. Furthermore, Owens and Wendt [15] introduced a semi-empirical formula:

$$\gamma_L(1 + \cos\theta) = 2\left(\sqrt{\gamma_S^d \gamma_L^d} + \sqrt{\gamma_S^p \gamma_L^p}\right), \tag{2}$$

where the superscripts d and p represent the dispersion and polar components, while the subscript S and L represent the solid and liquid. It can be seen from the above equation that, in order to calculate the solid surface free energy, the components of the surface free energies of the probe liquids must be known. The components of the two liquids reported in the literature are used here, as shown in Table 1. The contact angles and surface free energies of the samples are shown in Table 2. It can be seen from Table 2 that, mean contact angles of diiodomethane become a little larger, and the contact angles of water become much larger after coating with the DLC film. The surface free energies are reduced by coating with the DLC film.

3.4. Adhesion Force Measured by the Flat Tip

When using the flat tip, the samples used were grooved Si and DLC-coated grooved Si. 1089 uniformly distributed locations were selected in a scanning

TABLE 1 Surface Free Energy and Components of Probe Liquids

Probe liquid	γ_L (mJm^{-2})	γ_L^d (mJm^{-2})	γ_L^p (mJm^{-2})	References
Diiodomethane	50.8	48.5	2.3	[16]
Water	72.8	21.8	51.0	[17]

TABLE 2 Contact Angles and Surface Free Energies of the Samples

Sample	Diiodomethane (°)	Water (°)	γ_S^d (mJm^{-2})	γ_S^p (mJm^{-2})	γ_S (mJm^{-2})
Polished Si	33.8 ± 3.0	14.9 ± 5.7	27.5	43.5	71.0
Grooved Si	35.9 ± 1.9	21.9 ± 2.4	27.1	41.3	68.4
DLC-coated polished Si	35.2 ± 1.8	57.8 ± 1.9	33.0	16.5	49.5
DLC-coated grooved Si	38.2 ± 3.4	53.3 ± 1.2	30.5	20.5	51.0

area 60 μm × 60 μm. A force–displacement curve was recorded for each location. The maximum applied load is 220 ~ 300 nN, loading rate is 405 ~ 520 nNs^{-1}, and the dwell-in time is 0 s. The experiments were carried out in turn under ambient conditions (ambient temperature 23°C ± 1°C, relative humidity 50% ± 1%) and in dry nitrogen (ambient temperature 25°C ± 1°C, water content <0.1 ppm). Figure 7 shows adhesion force histograms of these samples under both conditions. Each of them exhibits a Gaussian-like distribution (fitting curves displayed in Fig. 7). Under ambient conditions, the ratio of the mean adhesion force of DLC-coated grooved Si to that of grooved Si is ~1/13. In dry nitrogen, the ratio of the mean adhesion force of DLC-coated grooved Si to that of grooved Si is ~1/6.

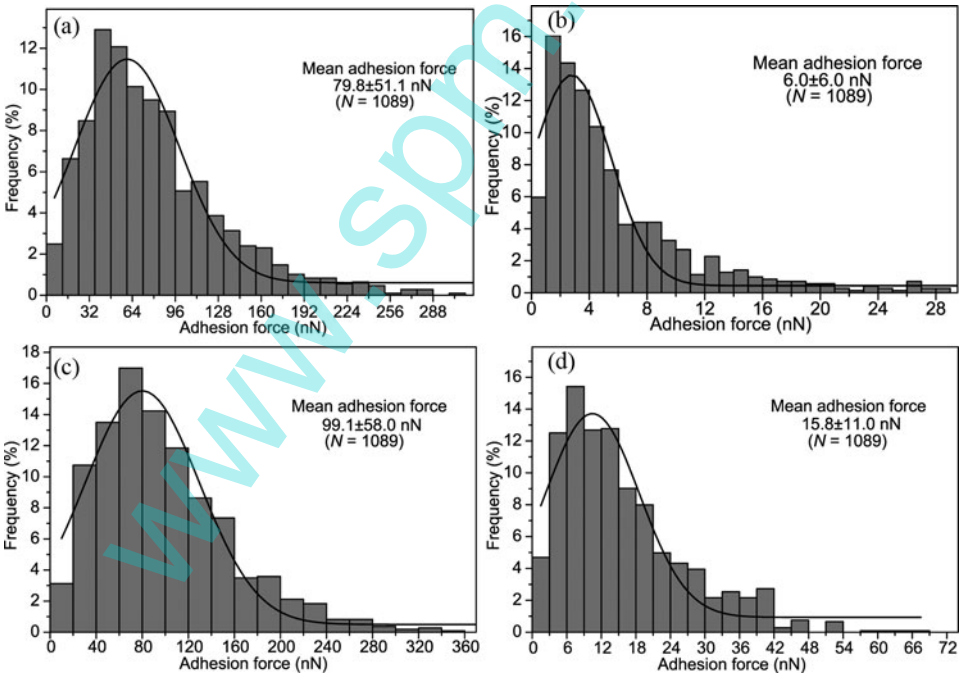

FIGURE 7 Histograms that show the distribution of adhesion force values by the flat tip: (a) grooved Si under ambient conditions, (b) DLC-coated grooved Si under ambient conditions, (c) grooved Si in dry nitrogen, and (d) DLC-coated grooved Si in dry nitrogen.

In dry gaseous environments, the vdW force and electrostatic force are the dominant forces. The contact between the flat tip and the sample is a multi-asperity contact. The multi-asperity contact consists of some single-asperity contacts. When a hard sphere with the radius R contacts with a flat surface, according to the Maugis-Dugdale (MD) model [18], the vdW force F_{ad} can be written as

$$F_{\mathrm{ad}} = (1.5 \sim 2)\pi R W_{12}, \tag{3}$$

where W_{12} is the work of adhesion. From Table 2, the surface free energies of the samples are reduced after coating with the DLC film. The decrease of the surface free energy will decrease the work of adhesion, leading to the lower adhesion force. For these samples, the mean adhesion forces in dry nitrogen are all larger than those under ambient conditions. This may be attributed to the electrostatic force in dry nitrogen, which leads to larger adhesion force.

Under ambient conditions, the capillary force is always present due to capillary condensation and adsorption of thin water films on surfaces. Moreover, it is assumed that the adhesion is mainly from the capillary force. In the case of a sphere with the radius R in contact with a flat surface, the capillary force can be written as [19]

$$F_{\mathrm{cap}} = 2\pi R\gamma_{\mathrm{W}}(\cos\theta_1 + \cos\theta_2), \tag{4}$$

where γ_{W} is the surface free energy of water, θ_1 and θ_2 are static contact angles of the tip and the sample with water, respectively. From Table 2, the water contact angles are increased after coating with the DLC film, leading to the lower capillary force.

In addition, the increase of roughness will reduce the real contact area, leading to lower adhesion force. The roughness of grooved Si increases a little after coating with the DLC film (from $R_{\mathrm{q}} = 36.6\,\mathrm{nm}$ to $R_{\mathrm{q}} = 40.9\,\mathrm{nm}$). Since the increase is small, the influence of roughness can be neglected.

3.5. Adhesion Force Measured by the Spherical Tip

When using the spherical tip to measure the adhesion force, four samples were used. 1089 uniformly distributed locations were selected in a scanning area $60\,\mu\mathrm{m} \times 60\,\mu\mathrm{m}$. A force–displacement curve was recorded for each location. The maximum applied load is $\sim$1200 nN, loading rate is $\sim$1800 nNs^{-1}, and the dwell-in time is 0 s. Figure 8 shows adhesion force histograms of these samples under ambient conditions (ambient temperature $23°\mathrm{C} \pm 1°\mathrm{C}$, relative humidity $45\% \pm 3\%$). Each of them exhibits a Gaussian-like distribution (fitting curves displayed in Fig. 8).

It can be seen from Fig. 8 that the ratio of the mean adhesion force of DLC-coated polished Si to that of polished Si is $\sim$1/47, while the ratio of the mean

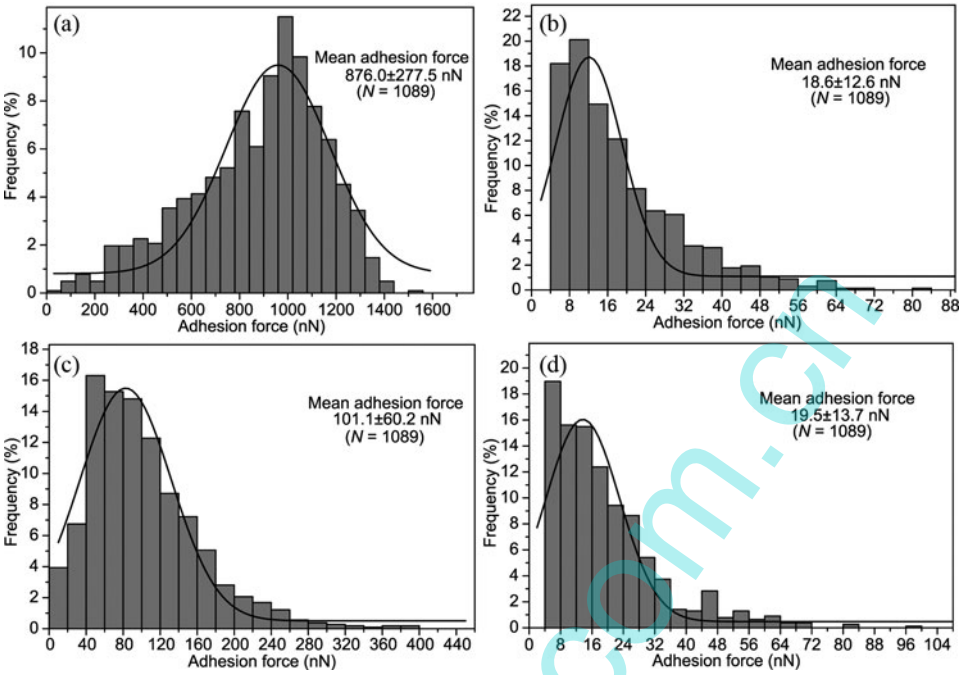

FIGURE 8 Histograms that show the distribution of adhesion by the spherical tip under ambient conditions for (a) polished Si, (b) DLC-coated polished Si, (c) grooved Si, and (d) DLC-coated grooved Si.

adhesion force of DLC-coated grooved Si to that of grooved Si is ~1/5. It can be seen from Fig. 6 that the roughness of DLC-coated polished Si is about eight times as large as that of polished Si. The increase of roughness largely reduces the real contact area, and eventually leads to lower adhesion force. When comparing Fig. 7 with Fig. 8, after coating with the DLC film, the mean adhesion force reduces to ~1/13 of that of grooved Si by using the flat tip, while the mean adhesion force reduces to ~1/5 of that of grooved Si by using the spherical tip. This difference may be attributed to the different contact geometries and materials. The materials of tips are silicon and silicon dioxide for both situations.

In dry nitrogen (ambient temperature 25°C ± 1°C, water content <0.2 ppm), the samples used were grooved Si and DLC-coated grooved Si. Figure 9 shows adhesion force histograms of these samples. Both of them exhibit Gaussian-like distributions (fitting curves displayed in the Fig. 9). In dry nitrogen, the ratio of the mean adhesion force of DLC-coated grooved Si to that of grooved Si is ~1/5.

3.6. Adhesion Force Measured by the Sharp Silicon Tips

When using sharp silicon tips, the samples used were polished Si and DLC-coated polished Si. The maximum applied load is ~300 nN, loading rate is ~600 nNs^{-1}, and the dwell-in time is 0 s. The sampling locations were

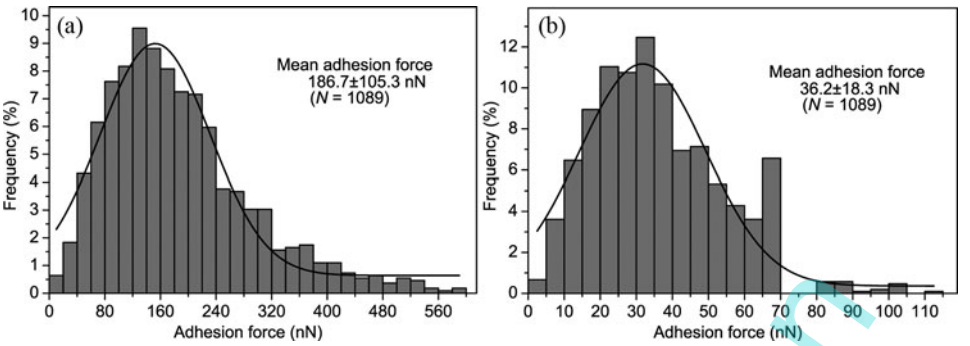

FIGURE 9 Histograms that show the distribution of adhesion force by using the spherical tip in dry nitrogen for (a) grooved Si and (b) DLC-coated grooved Si.

randomly selected in a scanning area 60 μm × 60 μm. In order to avoid serious wear, the number of the force–displacement curves was reduced.

The experiments of sharp silicon tip #1 were carried out in turn under ambient conditions (ambient temperature 23°C ± 1°C, relative humidity 43% ± 1%) and in dry nitrogen (ambient temperature 25°C ± 1°C, water content <0.1 ppm). 540 force–displacement curves were recorded by this tip. The relation of adhesion force and measurement number is shown in Fig. 10(a). The histograms of adhesion force all exhibit Gaussian-like distributions (not shown in Fig. 10). Under ambient conditions, the ratio of the mean adhesion force of DLC-coated polished Si (3.3 ± 2.6 nN) to that of polished Si (8.3 ± 2.1 nN) is ~2/5. In dry nitrogen, the ratio of the mean adhesion force of DLC-coated polished Si (4.7 ± 3.6 nN) to that of polished Si (41.2 ± 4.8 nN) is ~1/9.

It can be seen from Fig. 10(a) that the adhesion force of polished Si increases with the measurement number under ambient conditions. Since

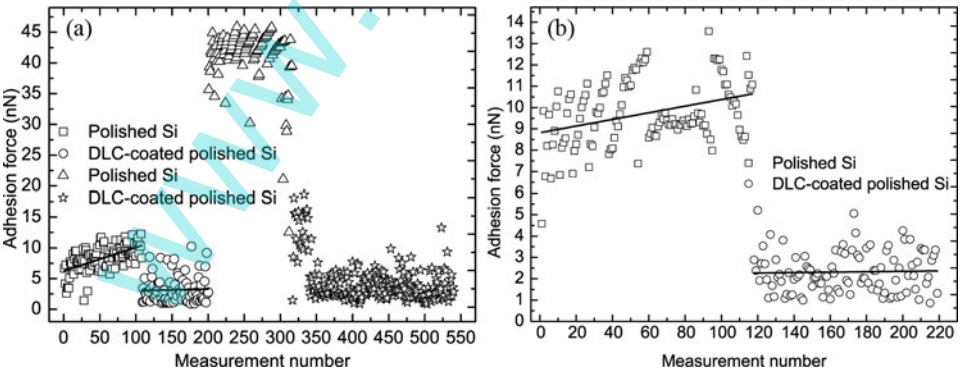

FIGURE 10 (a) Adhesion forces *vs.* sequential measurement number using the sharp silicon tip #1. The symbols □ and ○ represent data measured under ambient conditions, and the symbols △ and ☆ represent data measured in dry nitrogen. (b) Adhesion forces *vs.* sequential measurement number using the sharp silicon tip #2 in dry nitrogen.

the sampling points are randomly selected, this tip may wear in this process. Wear leads to the increase of the contact area between the tip and sample, resulting in larger adhesion forces. However, the adhesion force of DLC-coated polished Si shows no characteristic trend under ambient conditions. In dry nitrogen, the adhesion forces on polished Si are all large. The adhesion force remains relatively stable with the exception of some data. Adhesion forces on the DLC-coated polished Si are large at the beginning of the experiment. Then, the adhesion force becomes stable with the increase of the measurement number. On the whole, there is no tendency for either an increase or a decrease of the adhesion force with the increase of the measurement number for both samples in dry nitrogen.

The experiments of sharp silicon tip #2 were carried out in dry nitrogen (ambient temperature 25°C ± 1°C, water content <0.2 ppm). 219 force–displacement curves were recorded by this tip. The relation of adhesion force and measurement number is shown in Fig. 10(b). The histograms of adhesion force all exhibit Gaussian-like distributions (not shown in Fig. 10). The adhesion force of polished Si increases with the measurement number in dry nitrogen, while the adhesion force of DLC-coated polished Si shows no characteristic trend. The ratio of the mean adhesion force of DLC-coated polished Si (2.3 ± 1.0 nN) to that of polished Si (9.7 ± 1.5 nN) is ~1/4.

Figure 11 shows the SEM images of the sharp silicon tips before and after the experiments. After the experiments, the tips both show signs of

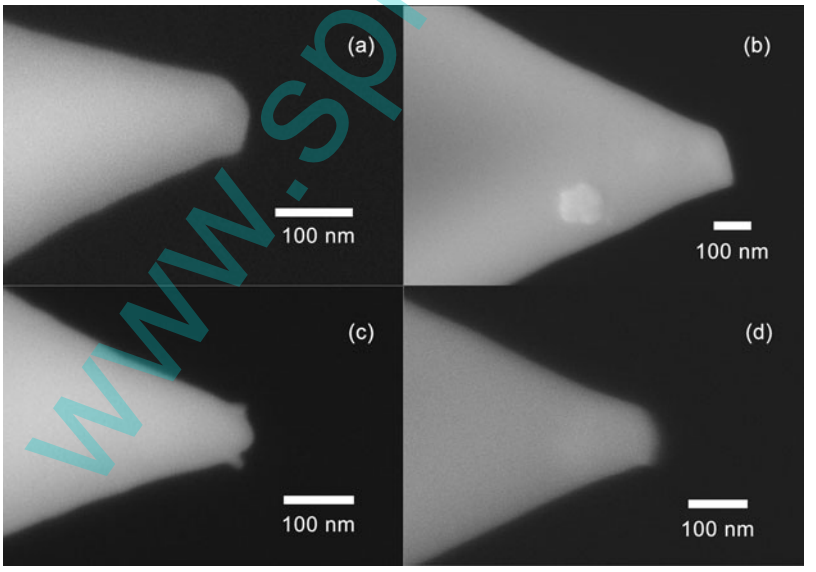

FIGURE 11 SEM images of the sharp tips (a) sharp tip #1 before the experiment, (b) sharp tip #1 after the experiment, (c) sharp tip #2 before the experiment, and (d) sharp tip #2 after the experiment.

wear. The wear of the sharp silicon tip #1 is more severe than that of the sharp silicon tip #2. There may be two reasons. On the one hand, more curves (540) were measured by the sharp silicon tip #1. On the other hand, tip #1 was used under ambient conditions. And tip wear increases with humidity [20].

In addition, the trends that adhesion force increases with the measurement number are obtained from the polished Si under both situations. It seems that the contact between silicon tip and silicon sample leads to more severe wear than the contact between silicon tips and the DLC film.

3.7. Adhesion Force Measured by the Sharp DLC-Coated Tips

When using sharp DLC-coated tips, the samples used were polished Si and DLC-coated polished Si. The maximum applied load is ~300 nN, loading rate is ~600 nNs^{-1}, and the dwell-in time is 0 s. The experiments were carried out under ambient conditions (ambient temperature 23°C ± 1°C, relative humidity 48% ± 1%) and in dry nitrogen (ambient temperature 25°C ± 1°C, water content <0.2 ppm). The sampling locations were randomly selected in a scanning area 60 μm × 60 μm. In order to avoid serious wear, the number of force–displacement curves for each tip for each sample is about 100.

The experiments of the sharp DLC-coated tip #1 were carried out under ambient conditions. 223 force–displacement curves were recorded by this tip. The relation of adhesion force and measurement number is shown in Fig. 12(a). The histograms of adhesion force all exhibit Gaussian-like distributions (not shown in Fig. 12). The ratio of the mean adhesion force of DLC-coated polished Si (2.2 ± 1.3 nN) to that of polished Si (5.1 ± 1.2 nN) is ~1/2. It can be seen from Fig. 12(a) that the adhesion force of polished Si increases with the measurement number under ambient conditions. Since the sampling points are randomly selected, this tip may wear in this process. Wear leads to the increase of the contact area between the tip and sample, resulting in larger adhesion forces. Since the thickness of the DLC coating is only ~15 nm, this film may have been worn. However, the adhesion force of DLC-coated polished Si shows no characteristic trend.

The experiments of the sharp DLC-coated tip #2 were carried out in turn under ambient conditions and in dry nitrogen. 316 force–displacement curves were recorded by this tip. The relation of adhesion force and measurement number is shown in Fig. 12(b). The histograms of adhesion force all exhibit Gaussian-like distributions (not shown in Fig. 12). It can be seen from Fig. 12(b), the adhesion force of DLC-coated polished Si increases with the measurement number under ambient conditions. However, the adhesion force of DLC-coated polished Si in dry nitrogen shows no characteristic trend. Then the adhesion force of polished Si in dry nitrogen increases with the measurement number again. Under ambient conditions, the mean adhesion force and the standard deviation are 1.9 ± 1.4 nN. In

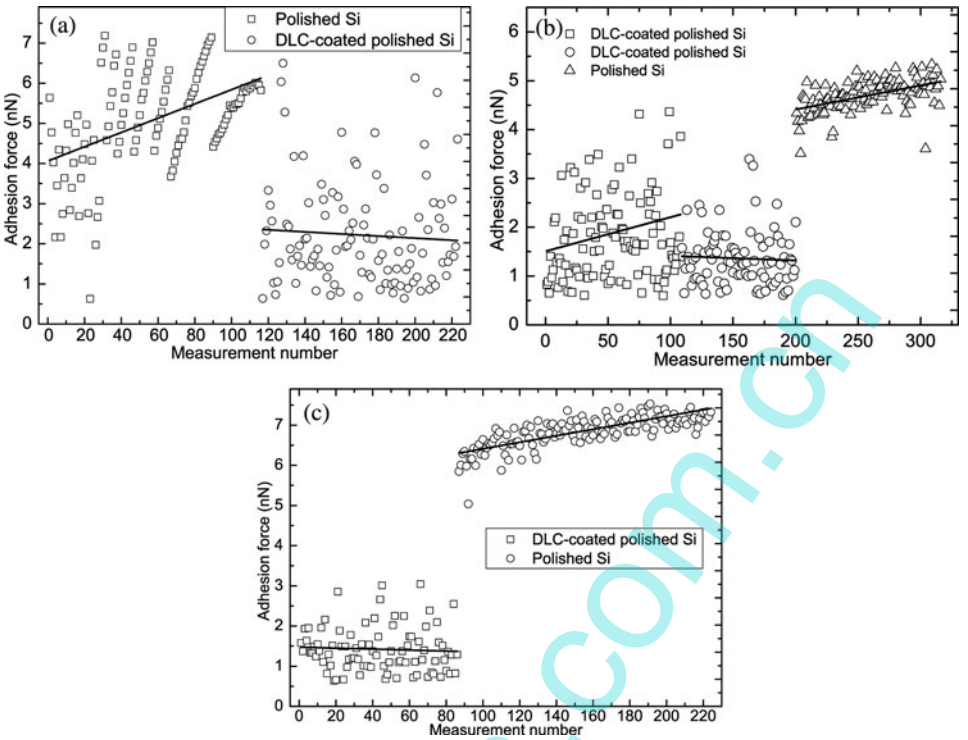

FIGURE 12 (a) Adhesion forces *vs.* sequential measurement number using the sharp DLC-coated tip #1 under ambient conditions. (b) Adhesion forces *vs.* sequential measurement number using the sharp DLC-coated tip #2. The symbol □ represents data measured under ambient conditions, and the symbols ○ and △ represent data measured in dry nitrogen. (c) Adhesion forces *vs.* sequential measurement number using the sharp silicon tip #3 in dry nitrogen.

dry nitrogen, the ratio of the mean adhesion force of DLC-coated polished Si (1.4 ± 0.5 nN) to that of polished Si (4.7 ± 0.3 nN) is ~2/7.

The experiments of the sharp DLC-coated tip #3 were carried out in dry nitrogen. 224 force–displacement curves were recorded by this tip. The relation of adhesion force and measurement number is shown in Fig. 12 (c). It can be seen from Fig. 12(c) that the adhesion force of DLC-coated polished Si shows no characteristic trend. However, the adhesion force of polished Si increases with the measurement number under ambient conditions. In dry nitrogen, the ratio of the mean adhesion force of DLC-coated polished Si (1.4 ± 0.6 nN) to that of polished Si (6.8 ± 0.5 nN) is ~1/5.

Figure 13 shows the SEM images of the sharp DLC-coated tips after the experiments. Usually, the tips have parabolic shapes. It can be seen from the figure that, the sharp DLC-coated tip #1 has been severely worn. The sharp DLC-coated tip #2 keeps the parabolic shape, since the wear is slight. The sharp DLC-coated tip #3 does not possess the parabolic shape any more, indicating some wear and tear.

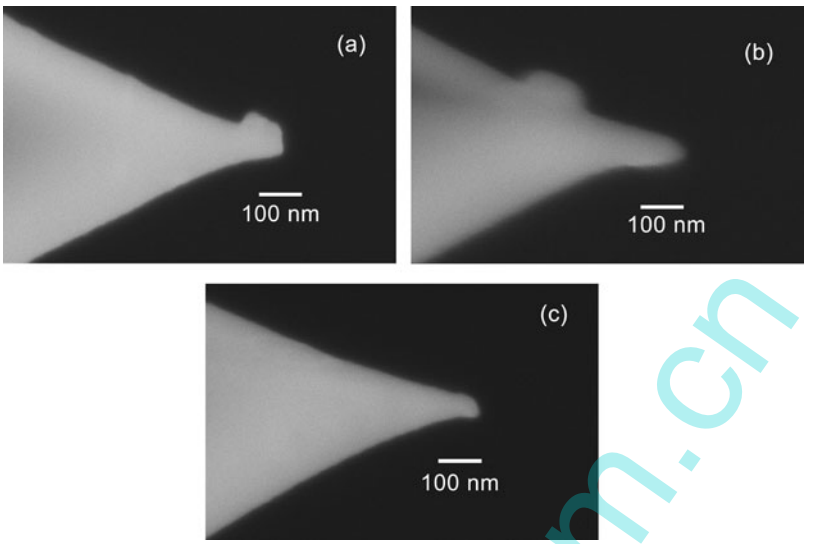

FIGURE 13 Scanning electron microscope images of the DLC-coated sharp tips after the experiments: (a) #1, (b) #2, and (c) #3.

3.8. Comparison of the Adhesion Forces

Table 3 shows the mean adhesion forces and standard deviations of the grooved Si and DLC-coated grooved Si. Table 4 shows the mean adhesion forces and standard deviations of the polished Si and DLC-coated polished Si. In these tables, the values in the brackets are the ratio of the mean adhesion force of DLC-coated sample to that of the original sample.

In Table 4, the symbol (↗) represents that the adhesion force increases with the measurement number, while (→) represents that the adhesion force remains stable with the measurement number. It can be seen from Table 4 that, the adhesion forces on the polished Si all increases with the measurement number under both conditions, with the exception of the adhesion forces measured by the sharp silicon tip #1 on the polished Si in dry nitrogen. Adhesion forces on the DLC-coated polished Si all remain stable with the measurement number under both conditions, with the exception of the adhesion force measured by the sharp DLC-coated tip #2 on the DLC-coated

TABLE 3 Mean Adhesion Forces and Standard Deviations of the Grooved Si and DLC-Coated Grooved Si

	Under ambient conditions		In dry nitrogen	
Tip types	Grooved Si (nN)	DLC-coated grooved Si (nN)	Grooved Si (nN)	DLC-coated grooved Si (nN)
Flat tip	79.8 ± 51.1	6.0 ± 6.0 (~1/13)	99.1 ± 58.0	15.8 ± 11.0 (~1/6)
Spherical tip	101.1 ± 60.2	19.5 ± 13.7 (~1/5)	186.7 ± 105.3	36.2 ± 18.3 (~1/5)

TABLE 4 Mean Adhesion Forces and Standard Deviations of the Polished Si and DLC-Coated Polished Si

Tip types	Under ambient conditions		In dry nitrogen	
	Polished Si (nN)	DLC-coated polished Si (nN)	Polished Si (nN)	DLC-coated polished Si (nN)
Spherical tip	876.0 ± 277.5	18.6 ± 12.6 (~1/47)	—	—
Sharp silicon tip #1	8.3 ± 2.1 (↗)	3.3 ± 2.6 (~2/5, →)	41.2 ± 4.8 (→)	4.7 ± 3.6 (~1/9, →)
Sharp silicon tip #2	—	—	9.7 ± 1.5 (↗)	2.3 ± 1.0 (~1/4, →)
Sharp DLC-coated tip #1	5.1 ± 1.2 (↗)	2.2 ± 1.3 (~1/2, →)	—	—
Sharp DLC-coated tip #2	—	1.9 ± 1.4 (↗)	4.7 ± 0.3 (↗)	1.4 ± 0.5 (~2/7, →)
Sharp DLC-coated tip #3	—	—	6.8 ± 0.5 (↗)	1.4 ± 0.6 (~1/5, →)

polished Si under ambient conditions. Since the sampling points are randomly selected, the increase of the adhesion force indicates the increase of the contact area between the tip and the sample. The increase of the contact area is caused by the wear of the tips. Thus, we can come to the conclusion that the DLC film not only reduces the adhesion, but also reduces wear under both conditions.

4. CONCLUSIONS

In this work, the effect of reducing adhesion of the DLC film is studied based on different contact geometries under ambient conditions and in dry nitrogen. The outcomes show that the adhesion distribution for each contact geometry exhibits a Gaussian-like distribution under both situations. Both under ambient conditions and in dry nitrogen, the DLC film can effectively reduce the adhesion force for different contact geometries. The reduction of the adhesion force was attributed to the decrease of the surface free energy and the increase of the contact angle for water. The surface roughness also takes effect on reducing the adhesion force in some experiments. The reduction ratio of adhesion is closely related to contact geometry, the roughness of DLC film, material characteristics paired with DLC film and the environment. And these factors are mutually coupled to determine the final reduction ratio. For the contact between the flat tip and a rough surface, the reduction ratio in dry nitrogen is larger than that under ambient conditions. For the contact between the spherical tip and a rough surface, the reduction ratios under ambient conditions and in dry nitrogen appear to be almost the

same. For single-asperity contact, the reduction ratio in dry nitrogen is larger than that under ambient conditions. Both under ambient conditions and in dry nitrogen, the DLC film also plays a role in reducing the wear and tear when measuring the adhesion forces.

FUNDING

This work was supported by the National Natural Science Foundation of China [Grant Number 51175182].

REFERENCES

[1] Kim, S. H., Asay, D. B., and Dugger, M. T., *Nano Today* **2**, 22–29 (2007).
[2] Zaghloul, U., Papaioannou, G., Bhushan, B., Coccetti, F., Pons, P., and Plana, R., *Microelectron. Reliab.* **51**, 1810–1818 (2011).
[3] Butt, H. J., Cappella, B., and Kappl, M., *Surf. Sci. Rep.* **59**, 1–152 (2005).
[4] Etsion, I., *J. Tribol.* **127**, 248–253 (2005).
[5] Amanov, A., Cho, I. S., Pyoun, Y. S., Lee, C. S., and Park, I. G. *Wear* **286–287**, 136–144 (2012).
[6] Maboudian, R. and Howe, R. T., *J. Vac. Sci. Technol.* **15**, 1–20 (1997).
[7] Houston, M. R., Howe, R. T., Komvopoulos, K., and Maboudian, R. *Mechanical Behavior of Diamond and Other Forms of Carbon Symposium*, (1995), pp. 391–402.
[8] Liu, H. and Bhushan, B., *J. Vac. Sci. Technol.* **21**, 1528–1538 (2003).
[9] Gou, L. Q., Shi, X. L., Zhao, X. M., Bai, Y., and Qiao, L. J., *Surf. Coat. Technol.* **206**, 4099–4105 (2012).
[10] Xie, J., Xie, H. F., Liu, X. R., and Tan, T. W., *Int. J. Mach. Tools Manuf.* **61**, 1–8 (2012).
[11] Chen, D., Wei, A., Wong, S., Peng, S., Xu, J., and Wilson, I. *J. Non-Cryst. Solids* **254**, 161–166 (1999).
[12] Müller, U. and Hauert, R., *Thin Solid Films* **290**, 323–327 (1996).
[13] Kaciulis, S., *Surf. Interface Anal.* **44**, 1155–1161 (2012).
[14] Fowkes, F. M., *J. Ind. Eng. Chem.* **56**, 40–52 (1964).
[15] Owens, D. K. and Wendt, R. C., *J. Appl. Polym. Sci.* **13**, 1741–1747 (1969).
[16] Shimizu, R. N. and Demarquette, N. R., *J. Appl. Polym. Sci.* **76**, 1831–1845 (2000).
[17] Barber, A. H., Cohen, S. R., and Wagner, H. D., *Phys. Rev. Lett.* **92**, 186103 (2004).
[18] Maugis, D., *J. Colloid Interface Sci.* **150**, 243–269 (1992).
[19] Bhushan, B. *Introduction to Tribology*, (Wiley, New York, 2002).
[20] Farshchi-Tabrizi, M., Kappl, M., Cheng, Y., Gutmann, J., and Butt, H.-J. *Langmuir* **22**, 2171–2184 (2006).